2 × 53 Gbit/s PAM-4 Transmission Using 1.3 μm DML With High Power Budget Enabled by Quantum-Dot SOA

Ahmed Galib Reza, Lakshmi Narayanan Venkatasubramani, *Member, IEEE*, Anil Raj Gautam, Prajwal D. Lakshmijayasimha, John O'Carroll, Richard Phelan, Diarmuid Byrne, Brian Kelly, *Member, IEEE*, Vladimir S. Mikhrin, Alexey Gubenko, *Member, IEEE*, and Liam P. Barry, *Senior Member, IEEE*

***Abstract*— We investigate the performance of 1.3 μm directly modulated multiple-quantum-well strained AlGaInAs distributed feedback laser in an optically amplified wavelength-division multiplexed (WDM) system for next-generation passive optical networks. We experimentally demonstrate 2 × 53 Gbit/s PAM-4 transmissions over 20 km of a single-mode fiber employing two 16-GHz bandwidth-limited directly-modulated lasers and compare the performance of quantum-well and quantum-dot semiconductor optical amplifiers (SOAs) in amplifying DWDM links. We successfully obtained the total power budget of 34 dB for each WDM channel using a quantum-dot SOA and 30-tap T-spaced feed-forward equalizer.**

***Index Terms*— Directly modulated laser, intensity modulation and direct detection, PAM-*m*, passive optical networks, quantum-well, quantum-dot, semiconductor optical amplifier, wavelength division multiplexing.**

I. Introduction

THE wavelength-division multiplexed (WDM) passive optical network (PON) is key to meeting the next-generation capacity requirements, which are exacerbated by the recent development of bandwidth-consuming technology and services such as 4K/8K video streaming, Internet-of-Things (IoT), artificial intelligence (AI), etc. [1]. As the International Telecommunication Union (ITU-T) is still working on the standardization and specifications of very high-seed PONs (VHSP) [2], [3], directly modulated lasers (DML) can still be the preferred choice for 50 Gbit/s/λ capacity high-speed PONs in the mid-term due to its simpler architecture, lower cost and power consumption, and higher optical output power [4], [5], [6], [7]. As the inherent adiabatic chirp of the DML can cause serious nonlinear distortions during transmissions through dispersive fibers, the O-band can be the optimum choice, as it offers nearly zero dispersion at 1310 nm at the cost of slightly higher attenuation coefficient compared with the C-band. The increased nonlinearity in the O-Band has resulted in the proposal for two-channel systems to minimize four-wave mixing issues in the fiber [8], [9]. Incorporation of higher-order modulation (HOM) formats such as 4 or 8-level pulse amplitude modulation (PAM-4/8) and advanced digital signal processing (DSP) techniques are also essential for the evolution of high-speed intensity-modulation and direct-detection (IM/DD) PON [10], [11]. As the PON system incurs significant passive losses and HOMs demand higher signal-to-noise ratio (SNR), optical amplifiers, specifically semiconductor optical amplifiers (SOAs) are ideally suited for signal amplification due to their small size and compatibility for integration with other components [12], [13].

The utilization of quantum dot (QD) SOAs in optical communications systems has gained significant interest as they can achieve faster gain recovery time, larger saturation power, lower noise figure, and patterning-free amplification [14], [15] when compared with conventional bulk or quantum well SOAs (QW-SOA). Recent demonstrations with a QD-SOA only discuss the amplification of single/WDM links with correlated data and ignore the impact of SOA nonlinearities and cross-gain modulation (XGM) during the amplification of uncorrelated data on adjacent channels [16], [17].

In this letter, we experimentally demonstrate 2 × 53 Gbit/s optically amplified WDM PAM-4 transmission in the O-band using 16 GHz bandwidth-limited DMLs over a 20 km single-mode fiber (SMF) for the PON continuous mode downstream transmission link. To extend the power budget, we utilize a high-gain QD-SOA and a conventional QW-SOA in the remote node (RN) or local exchange of a potential optically amplified WDM-PON. Besides, we

Received 19 August 2024; revised 21 October 2024; accepted 15 November 2024. Date of publication 22 November 2024; date of current version 2 December 2024. This work was supported in part by the Science Foundation Ireland under Grants 12/RC/2276_P2 and 23/IRDIFB/11955, in part by the European Union under European Innovation Council Projects 101136762 (UNICO) and 101137000 (MEngine), and in part by Enterprise Ireland under Grant DT 2019 0014A. *(Corresponding author: Ahmed Galib Reza).*

Ahmed Galib Reza, Lakshmi Narayanan Venkatasubramani, Anil Raj Gautam, and Liam P. Barry are with the School of Electronic Engineering, Dublin City University, Dublin 9, Ireland (e-mail: ahmed.galibreza@dcu.ie; lakshminarayanan.venkatasubramani@dcu.ie; anil.gautam4@mail.dcu.ie; liam.barry@dcu.ie).

Prajwal D. Lakshmijayasimha, Richard Phelan, Diarmuid Byrne, and Brian Kelly are with Eblana Photonics Ltd., West Pier Business Campus, Dublin, A96 A621 Ireland (e-mail: prajwal.d@eblanaphotonics.com; richard.phelan@eblanaphotonics.com; diarmuid.byrne@eblanaphotonics.com; brian.kelly@eblanaphotonics.com).

John O'Carroll was with Eblana Photonics Ltd., West Pier Business Campus, Dublin, A96 A621 Ireland. He is now with Scantinel Photonics, 89073 Ulm, Germany (e-mail: john.ocarroll@scantinel.com).

Vladimir S. Mikhrin and Alexey Gubenko are with Innolume GmbH, 44263 Dortmund, Germany (e-mail: vladimir.mikhrin@innolume.com; alexey.gubenko@innolume.com).

Color versions of one or more figures in this letter are available at https://doi.org/10.1109/LPT.2024.3504841.

Digital Object Identifier 10.1109/LPT.2024.3504841

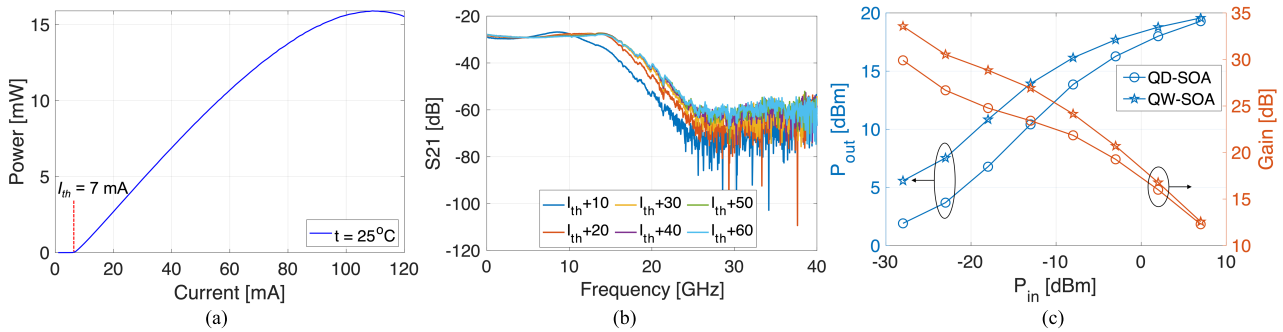

(a) (b) (c)

Fig. 1. (a) L-I characteristics of the DFB laser at 25°C. (b) Measured frequency response at different bias currents (in mA). (c) Output power and gain of the QD- and QW-SOA as a function of input power for a bias current of 500 mA.

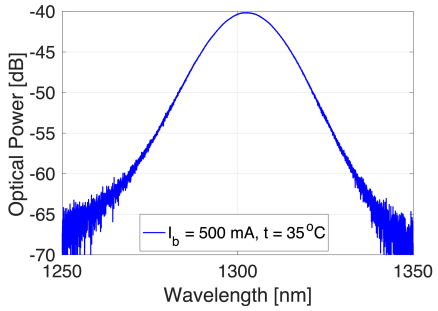

Fig. 2. Spectrum of the ASE noise of the QD-SOA.

compare the performance of the two SOA technologies in amplifying uncorrelated WDM links loaded with random PAM-4 data. We demonstrate that the QD-SOA can outperform the QW-SOA significantly in terms of bit error ratio (BER) and report a power budget in excess of 34 dB in each channel with a QD-SOA at the hard-decision low-density parity check (HD-LDPC) BER limit of 1×10^{-2}, which is adopted for 50G PON [18].

II. Device Characterization

The directly modulated distributed feedback (DFB) laser consists of a 150 μm long, and 2 μm wide ridge waveguide cavity. The active region contains a multi-QW strained AlGaInAs material designed for high-speed and uncooled operation. The DFB action is achieved using a 1st-order index coupled grating layer grown above the active region and designed for single-mode emission at 1310 nm. The light-current (L-I) curve of the fabricated DML is illustrated in Fig. 1(a). The threshold current of the DML is 7 mA (I_{th}) when operated at 25°C. Fig. 1(b) illustrates the S21 curves of the DMLs for various bias currents. We can see that the relaxation oscillation frequency of the laser increases with the bias current. From Figs. 1(a) and 1(b), we find that the DML generates an output power of ≈9.5 dBm and provides a 3 dB electro-optic (E/O) bandwidth of 16 GHz at a bias current of about 50 mA.

Fig. 1(c) illustrates the output powers and gains of the QD- and QW-SOAs as a function of the SOA input power when biased at 500 mA. We can see that the unsaturated gains of the QD- and QW-SOAs are about 30 dB and 33.5 dB for an input power of −28 dBm, respectively, and the gain compression is evident for both SOAs with the high input power. Fig. 2 shows the amplified spontaneous emission (ASE) spectrum of the QD-SOA against the wavelength. The SOA is biased at 500 mA and set to operate at 35°C. The center wavelength of the SOA is 1302.8 nm, which can be red-shifted by increasing the temperature, leading to a reduction in the SOA gain.

III. Experimental Setup

The experimental setup of the SOA-based optically amplified PON that simultaneously amplifies two wavelengths in the RN is illustrated in Fig. 3. A conceptual schematic of a WDM-PON is presented in Fig. 3(a), which broadcasts and amplifies multiplexed channels in the RN of a PON, potentially enables two-stage splitting in the networks and increases the number of supported users [20]. The performance of such a WDM-PON might be dominated by SOA-induced nonlinearity, ASE noise, and photodetector (PD) sensitivity. We utilize two parallel DMLs operating in the 1310 nm window. By changing the temperature of the thermoelectric cooler (TEC) from 17°C to 29.9°C, the wavelengths of the DMLs are tuned across 1310.9 nm to 1311.9 nm; realizing two-wavelength DWDM systems with channel spacings of 0.3 nm or 1 nm.

At the transmitter-side DSP, two independent 53 Gbit/s PAM-4 data streams are generated in MATLAB with a sequence length of 2^{16} symbols, which are 3.5 times upsampled to match the base clock frequency of 92.75 GSa/s of the arbitrary waveform generator (AWG). Subsequently, the PAM-4 symbol sequences are pulse-shaped by a root-raised cosine (RRC) filter with a roll-off factor of 0.1 and loaded to a two-channel AWG with 32 GHz analog bandwidth. We optimize the driving voltage of the two DMLs and set the peak-to-peak voltages of the AWG to 155 mV (channel-1) and 140 mV (channel-2), which are amplified by two 55 GHz RF amplifiers with gains of 22 dB. In the experiment, the biasing currents of the two DMLs are set to 54.95 mA and 50.35 mA, such that both DMLs could have symmetric optical output powers of about 9.5 dBm with extinction ratios of about 3.4 dB and 3.7 dB, respectively. Upon modulation, the outputs of the two DMLs are combined with a passive coupler and launched over a 20 km SMF with a total power of 9.5 dBm.

After fiber, conventional high-gain QW- and QD-SOAs are utilized to amplify both wavelengths simultaneously to boost the total power budget and compensate for transmission loss. A variable optical attenuator (VOA) is placed in the system before the SOA to vary the input power and also emulate the first stage splitting loss in the RN, which could potentially

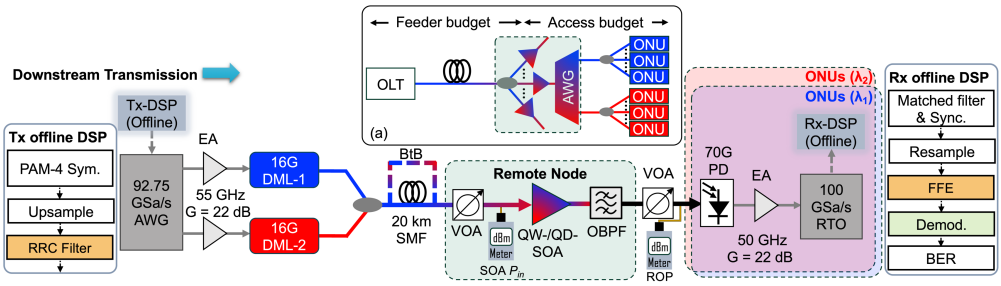

Fig. 3. Experimental setup for SOA-amplified 2 × 53 Gbit/s PAM-4 signals over 20 km. (a) Conceptual optically amplified WDM-PON architecture.

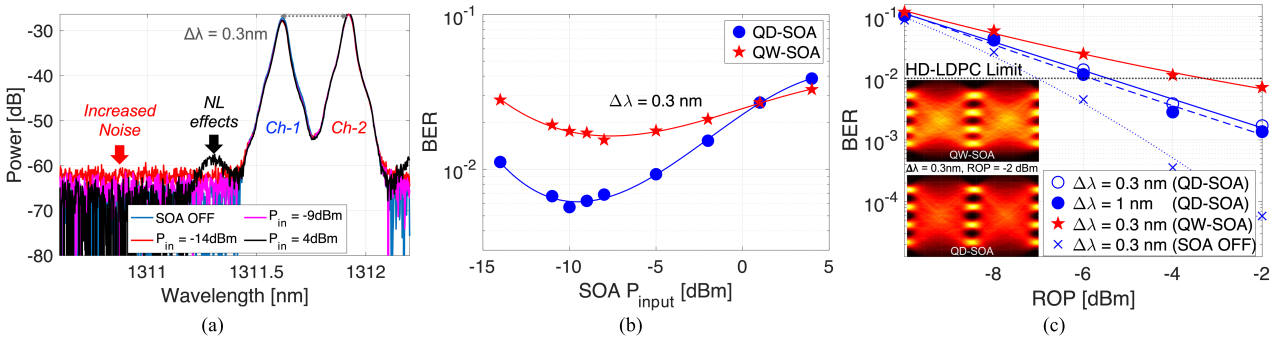

Fig. 4. (a) Optical spectra before and after optical amplification with a QD-SOA for a channel spacing of 0.3 nm. (b) BER of channel-2 (ch-2) at the ROP of −5 dBm versus input power into the QD - and $QW-SOA$. (c) BER as a function ROP after optically amplified BtB signal transmissions for various channel spacings with QD - and QW-SOAs. The inset shows equalized eye diagrams at $ROP = -2$dBm after amplifications with a QW-SOA and QD-SOA.

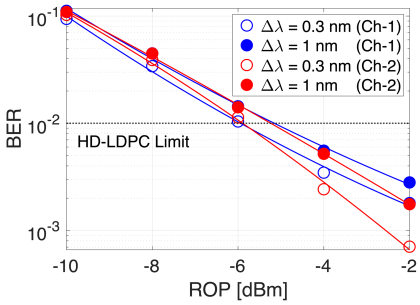

Fig. 5. BER versus ROP after optically amplified transmissions using a QD-SOA over 20 km SMF for various channel spacings.

contain SOAs, as shown in the proposed architecture in Fig. 3(a) [20]. Regardless of channel spacing, we demultiplex one of the amplified DWDM channels by setting the 3-dB bandwidth at ≈ 0.2 nm and tuning the central wavelength of the tunable optical bandpass filter (OBPF). The signal is then directly detected using a 70 GHz PD after adjusting the received optical power (ROP) with a VOA. Throughout the letter, the ROP is measured at the input of the PD, as shown in Fig. 3. The detected signal is amplified with a 50 GHz RF amplifier (22 dB gain) and captured using a 33 GHz real-time oscilloscope (RTO) operating at 100 GSa/s for offline processing. The receiver-side DSP includes RRC matched-filtering, resampling, synchronization, and a T-spaced 30-tap feed-forward equalizer (FFE). Finally, after PAM-4 symbol demodulation, the bit error ratio (BER) is measured.

IV. Experimental Results

Fig. 4(a) shows the optical spectra of the modulated DWDM signals in the case of back-to-back (BtB) transmission for a channel spacing of 0.3 nm, before and after amplifications using a QD-SOA for a fixed bias current of 500 mA and a constant temperature at 35°C. In the plot, the same power levels before and after the SOA are maintained with the help of a VOA after the SOA, this allows a direct comparison between the optical signal-to-noise ratio at the output and input of the amplifier. In the figure, the QD-SOA is operated for three different input powers of −14, −9, and +4 dBm. When the input power into the QD-SOA is low (−14 dBm), a significant increase in the noise floor due to ASE noise is observed. At a high input power of +4 dBm, the SOA exhibits gain saturation and nonlinearities, as new frequency components are found in the spectrum. At an input power of −9 dBm, the trade-off is optimal between the ASE noise and the SOA nonlinearities.

Fig. 4(b) shows the BERs of Ch-2 (1311.9 nm) at an ROP of −5 dBm for various input powers into the QD- and QW-SOAs after DWDM transmissions with a channel spacing of 0.3 nm over a BtB link. The QD-SOA outperforms the QW-SOA for input powers ranging from −14 dBm to −2 dBm. This could be due to inhomogeneous gain broadening, lower ASE, higher saturation power, and patterning-free amplification with a QD-SOA during 26.5G transmissions due to its faster gain recovery time compared with a QW-SOA, resulting in lower nonlinear penalties and XGM-induced crosstalk in DWDM systems [19]. For both SOAs, the best performances are achieved for input powers of between −8 dBm and −10 dBm due to ideal SOA operating conditions considering the ASE and nonlinearity.

Fig. 4(c) shows the BERs of Ch-2 (1311.9 nm) as a function of ROPs after unamplified and amplified DWDM BtB transmission experiments with QD- and QW-SOAs. In the experiment, the input powers are set to −9 and −8 dBm for the QD- and QW-SOAs, respectively. It can be seen that the QD-SOA outperforms the QW-SOA quite significantly for any

ROPs due to lower XGM and other SOA nonlinear penalties. Depending on the channel spacing, the QD-SOA system suffers around 1-1.5 dB penalty at the HD-LDPC BER threshold level in contrast to the unamplified system, which is expected due to the absence of SOA-induced ASE noise and nonlinearities in an unamplified transmission. On the other hand, the QW-SOA system exhibits about a 3.4 dB penalty at the same pre-FEC BER level. We note that when the channel spacings are increased to 1 nm, there are only marginal improvements in the BER performances for the QD-SOA, as the wider channel spacing does not ease the impact of ASE noise and XGM-induced crosstalk. In the insets, the equalized eye diagrams of the QW-SOA and QD-SOA amplified signals are shown at an ROP of -2 dBm after BtB transmissions. As expected, the SOA nonlinearities are more pronounced in the eye diagram for the QW-SOA, whereas clear eye openings are observed for the QD-SOA; demonstrating the effectiveness of QD-SOA in significantly reducing the patterning effects and XGM.

In Fig. 5, we plot the BER results of QD-SOA amplified DWDM channels as a function of ROP after transmissions over a 20 km SMF. We can observe that both channels can reach the HD-LDPC level BER threshold of 1×10^{-2}. Regardless of channel spacing, channel-2 (1311.9 nm) always performs slightly better than channel-1, which is tuned either at 1310.9 or 1311.6 nm. This could be due to the SOA gain profile or slightly different RIN or bandwidth levels for the two DMLs utilized in the experiment. At an ROP of -6 dBm, both channels can guarantee at least the HD-LDPC level BER performances, providing a total power budget of >34 dB. Compared with the BtB case (Fig. 4(c)), no significant differences are observed in the BER performance. We note that the total power budget of the PON is calculated by adding the feeder and access budget [21], [22], which can also be obtained by subtracting the receiver sensitivity at the HD-LDPC level BER from the signal launch power to the fiber and adding the SOA gain of 22 dB for an SOA input signal power of -9 dBm.

V. Conclusion

In this letter, we have demonstrated optically amplified 2×53 Gbit/s DWDM PAM-4 transmissions over 20 km using 16 GHz O-band DMLs. By utilizing a high-gain QD-SOA and simple DSP techniques, we report a >34 dB power budget on each WDM channel that can be utilized to accommodate large splitting ratios or to support next-generation long-reach PON. The monolithically integrable optical transceivers and amplifiers explored in this letter can potentially contribute to the development of high-capacity, power-efficient, and long-reach PONs.

Acknowledgment

Views and opinions expressed are however those of the author(s) only and do not necessarily reflect those of the European Union. Neither the European Union nor the granting authority can be held responsible for them.

References

[1] J. Zhang and Z. Jia, "Coherent passive optical networks for 100G/λ-and-beyond fiber access: Recent progress and outlook," *IEEE Netw.*, vol. 36, no. 2, pp. 116–123, Mar. 2022.

[2] *PON Transmission Technologies Above 50 Gb/s Per Wavelength*, ITU-T Recommendation, Geneva, Switzerland, 2023.

[3] I. B. Kovacs, M. S. Faruk, P. Torres-Ferrera, and S. J. Savory, "Simplified coherent optical network units for very-high-speed passive optical networks," *J. Opt. Commun. Netw.*, vol. 16, no. 7, p. C1, 2024.

[4] *Higher Speed Passive Optical Networks*, document G.9804, ITU-T Recommendation, 2021.

[5] A. G. Reza and J.-K.-K. Rhee, "Nonlinear equalizer based on neural networks for PAM-4 signal transmission using DML," *IEEE Photon. Technol. Lett.*, vol. 30, no. 15, pp. 1416–1419, Aug. 1, 2018.

[6] J. Nie et al., "A novel adaptive PWL equalizer using soft-partition for DML-based PAM-6 transmission," *J. Lightw. Technol.*, vol. 42, no. 8, pp. 2744–2751, Apr. 15, 2024.

[7] A. G. Reza, M. Troncoso-Costas, C. Browning, F. J. Diaz-Otero, and L. P. Barry, "Single-lane 54-Gbit/s PAM-4/8 signal transmissions using 10 G-class directly modulated lasers enabled by low-complexity nonlinear digital equalization," *IEEE Photon. J.*, vol. 14, no. 3, pp. 1–9, Jun. 2022.

[8] S. Deligiannidis, A. Bogris, C. Mesaritakis, and Y. Kopsinis, "Compensation of fiber nonlinearities in digital coherent systems leveraging long short-term memory neural networks," *J. Lightw. Technol.*, vol. 38, no. 21, pp. 5991–5999, Nov. 1, 2020.

[9] S. Deligiannidis, A. Bogris, C. Mesaritakis, and Y. Kopsinis, "Dispersion tolerant 200 Gb/s dual-wavelength IM/DD transmission with 33dB link budget for next generation PON," in *Proc. 49th Eur. Conf. Opt. Commun. (ECOC)*, Glasgow, U.K., 2023, pp. 1091–1094.

[10] A. Galib Reza, M. Troncoso-Costas, L. P. Barry, and C. Browning, "4×75-Gbit/s optically amplified WDM-PON with beyond 31-dB power budget employing PAM-4 transmission and a recurrent neural network," in *Proc. Eur. Conf. Opt. Commun. (ECOC)*, Basel, Switzerland, Sep. 2022, pp. 1–4.

[11] G. Caruso, I. N. Cano, D. Nesset, G. Talli, and R. Gaudino, "Real-time 100 Gb/s PAM-4 for access links with up to 34 dB power budget," *J. Lightw. Technol.*, vol. 41, no. 11, pp. 3491–3497, Jun. 1, 2023.

[12] C. Caillaud et al., "Monolithic integration of a semiconductor optical amplifier and a high-speed photodiode with low polarization dependence loss," *IEEE Photon. Technol. Lett.*, vol. 24, no. 11, pp. 897–899, Jun. 1, 2012.

[13] L. N. Venkatasubramani, A. G. Reza, and L. Barry, "On the application of semiconductor optical amplifier towards terabit/s short-reach IM/DD transmission systems," *Proc. SPIE*, vol. 12894, pp. 70–73, Mar. 2024.

[14] T. Akiyama, M. Sugawara, and Y. Arakawa, "Quantum-dot semiconductor optical amplifiers," *Proc. IEEE*, vol. 95, no. 9, pp. 1757–1766, Sep. 2007.

[15] A. Hamié, M. Hamze, J. L. Wei, A. Sharaiha, and J. M. Tang, "Theoretical investigations of quantum-dot semiconductor optical amplifier enabled intensity modulation of adaptively modulated optical OFDM signals in IMDD PON systems," *Opt. Exp.*, vol. 19, no. 25, p. 25696, 2011.

[16] L. N. Venkatasubramani, A. G. Reza, V. S. Mikhrin, A. Gubenko, A. R. Kovsh, and L. Barry, "100 gbps PAM4 transmissions over 50 km with 40 dB power budget for PON using a high-gain quantum dot SOA," in *Proc. Opt. Fiber Commun. Conf. (OFC)*, San Diego, CA, USA, 2024, pp. 1–3, Paper Th2A.6.

[17] C. St-Arnault et al., "Performance comparison of QD-SOA, QW-SOA, bulk-SOA and PDFA for multi-tbps O-band WDM links," in *Proc. Opt. Fiber Commun. Conf. (OFC)*, San Diego, CA, USA, 2024, pp. 1–3, Paper M3E.5.

[18] *50-Gigabit-capable Passive Optical Networks (50G-PON): Physical Media Dependent (PMD) Layer Specification*, Standard G.9804.3, ITU-T Recommendation, 2021.

[19] M. Matsuura and N. Kishi, "Multichannel transmission of intensity- and phase-modulated signals by optical phase conjugation using a quantum-dot semiconductor optical amplifier," *Opt. Lett.*, vol. 38, no. 10, p. 1700, 2013.

[20] Fujitsu Ltd. (2011). *Fujitsu Develops Optical Amplifier Technology for Next Generation Optical Access Systems*. Accessed: Oct. 4, 2024. [Online]. Available: https://www.fujitsu.com/global/about/resources/news/press-releases/2011/1013-03.html

[21] F. Saliou et al., "Reach extension strategies for passive optical networks [Invited]," *J. Opt. Commun. Netw.*, vol. 1, no. 4, pp. C51–C60, 2009.

[22] A. Emsia, Q. T. Le, M. Malekizandi, D. Briggmann, I. B. Djordjevic, and F. Küppers, "WDM–TDM NG-PON power budget extension by utilizing SOA in the remote node," *IEEE Photon. J.*, vol. 6, no. 2, pp. 1–10, Apr. 2014.